Science of the Total Environment 646 (2019) 564–572

Contents lists available at ScienceDirect

Science of the Total Environment

journal homepage: www.elsevier.com/locate/scitotenv

Aerosols in an arid environment: The role of aerosol water content, particulate acidity, precursors, and relative humidity on secondary inorganic aerosols

Haiting Wang [a,b], Jing Ding [a], Jiao Xu [a], Jie Wen [a], Jianhong Han [c], Keling Wang [c], Guoliang Shi [a,*], Yinchang Feng [a], Cesunica E. Ivey [d], Yuhang Wang [e], Athanasios Nenes [e,f], Qianyu Zhao [a], Armistead G. Russell [g]

[a] State Environmental Protection Key Laboratory of Urban Ambient Air Particulate Matter Pollution Prevention and Control, Center for Urban Transport Emission Research, College of Environmental Science and Engineering, Nankai University, Tianjin, China
[b] National Academy for Mayors of China, Beijing, China
[c] Hohhot Environmental Monitoring Center, China
[d] Department of Chemical and Environmental Engineering, University of California Riverside, Riverside, CA, USA
[e] Earth and Atmospheric Sciences, Georgia Institute of Technology, Atlanta, GA, USA
[f] School of Architecture, Civil and Environmental Engineering, École Polytechnique Fédérale de Lausanne, Lausanne, CH-1015, Switzerland
[g] School of Civil and Environmental Engineering, Georgia Institute of Technology, Atlanta, GA, USA

HIGHLIGHTS

- Secondary aerosol in Hohhot was low.
- Aerosol pH was estimated by a thermodynamic equilibrium model.
- Multiple receptor models were used to explore the source contributions.
- Aerosol water content and particulate acidity were positively associated with secondary SO_4^{2-}.
- NO_2 and RH had a significant impact on secondary NO_3^- in an arid atmosphere.

GRAPHICAL ABSTRACT

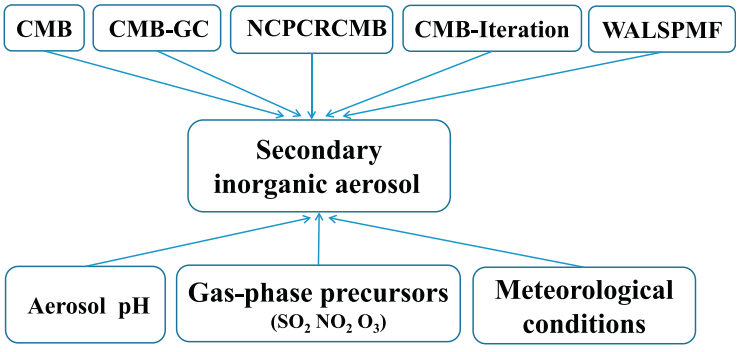

ARTICLE INFO

Article history:
Received 25 May 2018
Received in revised form 21 July 2018
Accepted 23 July 2018
Available online 24 July 2018

Editor: Jianmin Chen

Keywords:
Seasonal variations
Statistical relationship
Meteorological conditions
Five receptor models
Secondary inorganic aerosol

ABSTRACT

Meteorological conditions, gas-phase precursors, and aerosol acidity (pH) can influence the formation of secondary inorganic aerosols (SIA) in fine particulate matter ($PM_{2.5}$). Most works related to the influence of pH and gas-phase precursors on SIA have been laboratory research, but field observation research is very scarce, especially in arid environments. The relationship among SIA, pH, gas-phase precursors, and meteorological conditions are investigated in Hohhot, a major city in China with an arid environment. Secondary inorganic species, e.g., SO_4^{2-}, NO_3^-, were typically found at low levels, reflecting the low level of secondary aerosol. It is interesting to note that the level of SO_2 in Hohhot was higher than in other cities while SO_4^{2-} was relatively lower than in other cities. Multiple receptor models were used to explore the contributions to the SIA and quantify the source impacts on the SIA. Annual average aerosol pH in Hohhot was 5.6 (range 1.1–8.4) which was estimated by a thermodynamic equilibrium model. Additionally, a statistical method was used to evaluate the influence of SIA sources on ambient aerosol concentrations. Aerosol water content and particulate acidity were found to be positively associated with secondary SO_4^{2-}, while NO_2 and RH had a significant impact on secondary NO_3^- in an arid atmosphere. The

* Corresponding author.
E-mail address: nksgl@nankai.edu.cn (G. Shi).

https://doi.org/10.1016/j.scitotenv.2018.07.321

findings explain the relationship between gaseous precursors, relative humidity, aerosol pH and temperature in the arid city of Hohhot.

1. Introduction

With the rapid industrialization and urbanization in China and abroad, air quality is declining rapidly around the world which has made research on atmospheric aerosols important increasingly. Atmospheric aerosols can be classified into two types: primary aerosol and secondary aerosol (Chowdhury et al., 2007). Primary aerosols are emitted from various anthropogenic and natural sources directly such as vehicle exhaust, coal combustion, crustal dust, and cement. Secondary aerosols, are formed through gas-to-particle transformation processes and oxidizing reactions, such as a sulfate or nitrate (Xue et al., 2016; Jaiprakash et al., 2017). High particulate matter (PM) levels and haze events are dominated by secondary inorganic aerosol (SIA) pollution (Mysliwiec and Kleeman, 2002; Wang et al., 2014a, 2014b), which is produced from gas-phase precursors, especially sulfur dioxide (SO_2), nitrogen oxides (NO_x), and ammonia (NH_3) (Huang et al., 2010; Zhang et al., 2013). SIA have a strong effect on the hygroscopicity and acidity of aerosols which could influence aerosol-phase chemistry and the uptake of gas-phase species by particles (Xue et al., 2011; Shon et al., 2012). In the formation of SIA meteorological conditions (temperature, wind speed, and humidity) and gas-phase precursors were important factors (Pun and Seigneur, 2001; Wang et al., 2015; Han et al., 2016). Wang et al. (2014a, 2014b) concluded that during the haze episodes in the Jing-Jin-Ji area, sustained weak wind, growing humidity, and continuously high humidity conditions were the leading meteorological causes for severe pollution levels. Temperature was connected to the rates of the SO_2 oxidation and the formation of secondary sulfate (Ronneau, 1987; Seinfeld and Pandis, 2006). Temperature also affects the partitioning of nitrate (NO_3^-) in the atmospheric fine and coarse fraction of aerosols (Wakamatsu et al., 1996; Han et al., 2016). Higher humidity can create favorable conditions for aqueous reactions and lead to the formation of SIA (Han et al., 2016). Moreover, during higher relative humidity (RH) conditions, nitric acid (HNO_3) and ammonia (NH_3) can be dissolved, and particulate NO_3^- and ammonium (NH_4^+) formation may accelerate (Trebs et al., 2004, 2005; Han et al., 2016). Furthermore, SO_2, NO_2, and O_3 are precursors of SIA, and these precursors have close relationships with the formation of SIA (Pun and Seigneur, 2001; Amil et al., 2016).

Cheng et al. (2016) showed that in the relative alkaline condition in Beijing, nitrogen may promote the secondary sulfate formation including field observation and modelling study. Tie et al. (2017) investigated the positive feedback loop between SIA and meteorology. However, the SIA studies focused on the arid regions in China, Hohhot was rare. As the typical arid region in China (the annual RH was <50%), the geographic location of Hohhot (the capital and center of Inner Mongolia) was specific, the Köppen climate classification for Hohhot is also cold semi-arid climate, the pollution source characteristics, the RH, the dust period in Hohhot were different from Beijing and other northern regions, the level of SIA formation can be very different compared to other regions. So it is essential to explore the level of SIA, the influence of meteorological conditions and precursors on SIA in Hohhot.

To further address the relation among pH, gaseous precursors, and meteorological conditions of secondary sulfate, the level of secondary aerosol should be analyzed first. Receptor models are commonly used to apportion the contribution of SIA. For aerosol pH, because it is difficult to measure directly (Song et al., 2018), a thermodynamic equilibrium model (ISORROPIA-II) was used to predict pH in this study. ISORROPIA-II was also used to estimate other characteristics of aerosol such as water content. Here three items were investigated. First, 1) concentrations of $PM_{2.5,}$ which represented the four different seasons, were obtained by the offline filter sampling, and the corresponding meteorological conditions and levels of gas-phase pollutants (WS, RH, T, NO_2, SO_2, O_3) in Hohhot were also acquired. Next, 2) aerosol pH was investigated using ISORROPIA-II, and receptor models were used for source identification. Finally, 3) statistical methods were employed to analyze the relative influence of meteorological conditions, gas-phase precursors, and aerosol pH on the SIA to understand the formation of SIA in Hohhot. The findings in this work can provide useful information regarding formation mechanisms of SIA in arid environments.

2. Materials and methods

2.1. Study area

Hohhot, an arid city located in central Inner Mongolia, northern China, has typical continental climate with high winds and little rain in spring (Fig. S1). The diurnal maximum wind speed can typically about 10 m/s which may result in periods of high wind-blown dust. The annual precipitation is 390 mm, with most of the precipitation occurring in July and August, and this is much lower than the annual evaporation capacity of 2000 mm, so the ground is typically dry. High winds contribute to the arid environment. The power industry accounts for a majority of the total coal consumption in Hohhot. The heating period in Hohhot begins in mid-October and ends around mid-April the following year.

2.2. ISORROPIA II

ISORROPIA-II is a thermodynamic equilibrium model that predicts equilibrium partitioning of species (Na^+, Ca^{2+}, Mg^{2+}, K^+, NH_4^+, SO_4^{2-}, NO_3^-, Cl^-) between the gas and particle phases using measured particulate species to evaluate fine particle pH levels (Tian et al., 2013a, 2013b). Model inputs include gas and particle concentrations of species that affect the value of pH (Fang et al., 2017). In this study, ISORROPIA-II was run in the forward mode and "metastable" phase state, but NH_3 was not included. Further information about ISORROPIA-II can be obtained in other studies (Guo et al., 2015, 2016; Weber et al., 2016).

2.3. Meteorological parameters, gas-phase pollutants, and air mass back trajectories

The datasets of meteorological parameters and gas-phase pollutants were obtained online using https://www.wunderground.com/ and http://www.aqistudy.cn/, respectively, to identify the seasonal variations of meteorological parameters and gas-phase pollutants during the sampling period in Hohhot. The analysis of air mass back trajectories was dependent on the TrajStat, a geographic information system (GIS) software that uses various trajectory statistical analysis methods to identify potential aerosol sources from long-term air pollution measurement data (http://www.meteothinker.com/Downloads.html). The meteorological data used in this model was downloaded at http://www.arl.noaa.gov/HYSPLIT.php (including horizontal and vertical wind speed, temperature, pressure, relative humidity, precipitation, etc.). In this study, two-day air mass back trajectories were calculated every 6 h using the TrajStat model initiated at 1000 m above ground level, located at 111.41° east longitude and 40.48° north latitude (the center of Hohhot). The related analysis by TrajStat model can be seen in the Supplementary Information.

2.4. Receptor models for source impact analysis

Previous studies have found that individual models may have weaknesses and uncertainties (Shi et al., 2011b; Tian et al., 2013a, 2013b). In this study, five models including Chemical Mass Balance (CMB), Chemical Mass Balance-Gas Constraint (CMB-GC), Nonnegative Constrained Principal Component Regression Chemical Mass Balance (NCPCRCMB), Chemical Mass Balance-Iteration (CMB-Iteration) model, and Weighted Alternating Least Squares-Positive Matrix Factorization (WALSPMF) were all used at the same time to avoid the inaccuracy of a single model to analyze the contribution of local pollution sources (including secondary sources) to SIA concentrations.

Receptor models play a major role in source impact analyses and are widely used in atmospheric studies. CMB is a commonly-used receptor model which takes into account the chemical composition of ambient samples to evaluate the influence of different pollution sources on the concentrations of pollutants (Morino et al., 2011; Hopke, 2003). Different pollution sources have unique ratios of chemical components, and these characteristics make up a profile of the different sources and are the basis for model calculations and source identification. Multiple models were applied in this study to address the weaknesses of the individual models. One model, CMB-GC, is an extension of the traditional CMB model that uses gas phase concentrations to set additional constraints, and it can be applied to estimate the contribution of sources to particulate matter. More information about CMB-GC can be found in Marmur et al. (2005) and Zhai et al. (2016). The NCPCRCMB model included the principle component regression (PCR) route in the CMB model and was developed to solve the collinearity problem for source impact analysis. The principle of NCPCRCMB is described in detail in a previous study (Tian et al., 2013a, 2013b). CMB-Iteration is a new method used to estimate SOC based on the traditional CMB model and estimates the concentration of SOC and the contribution of the sources directly without using an SOC profile. The detailed algorithm of the CMB-Iteration model is described in Shi et al. (2011a). In the factor analysis model (FA), source profile information is not needed since the FA model can distinguish the temporal variability of different sources. WALSPMF was introduced in a previous study as a new FA model which combined an eigenvalue-based method and weighted alternating least squares (WALS) process and distinguished different sources more reasonably. Furthermore, WALSPMF has been developed to identify the impact of possibly unidentified sources (Shi et al., 2016). The interfaces of afore-mentioned models can be seen in Figs. S2–S5, and the models can be obtained at (http://env.nankai.edu.cn/air/list/?110_1.html or http://russellgroup.ce.gatech.edu/node/16?destination=node/16).

3. Results and discussion

3.1. Concentrations of $PM_{2.5}$, chemical components, and gas-phase precursors

The concentrations of $PM_{2.5}$ in Hohhot are shown in Table 1. The daily $PM_{2.5}$ concentration ranged from 13 to 284 μg m^{-3}, and the annual $PM_{2.5}$ mass concentration was 66 μg m^{-3}. Compared to the ambient air quality standard in China, The concentrations in Hohhot were nearly twice as high as the Chinese standard (35 μg m^{-3}) but lower than most of the provincial capitals in northern China (the most polluted Beijing-Tianjin-Hebei Region, Beijing 81 μg m^{-3} (2015), Tianjin 81 μg m^{-3} (2015), and Shijiazhuang 105 μg m^{-3} (2015)). Hohhot $PM_{2.5}$ levels were compared to other cities such as Veneto, Italy (low wind speeds and stable atmospheric stratification, 33 μg m^{-3}) (Squizzato et al., 2012) and Osaka, Japan (the commercial and industrial city, 13–35 μg m^{-3}) (Sasaki and Sakamoto, 2005), where their concentrations of $PM_{2.5}$ were much lower than Hohhot. This may indicate heavy fine particulate matter pollution in China.

The annual contents of major chemical components in $PM_{2.5}$ are also listed in Table 1. The components ranked as follows: OC (14 μg m^{-3}; 18%), SO_4^{2-} (7.3 μg m^{-3}; 11.0%), NO_3^- (4.1 μg m^{-3}; 6.3%), EC (4.0 μg m^{-3}; 5.7%), Si (3.9 μg m^{-3}; 6.1%), NH_4^+ (3.3 μg m^{-3}; 5.0%), Ca (2.6 μg m^{-3}; 4.9%), Al (2.5 μg m^{-3}; 4.0%), Cl^- (1.6 μg m^{-3}; 2.3%), K (1.1 μg m^{-3}; 1.7%), and Fe (1.1 μg m^{-3}; 1.5%). The measured chemical composition constituted over 70% of $PM_{2.5}$ mass. The comparisons of secondary species in different cities are listed in Table S1. The secondary species (SO_4^{2-} and NO_3^-) in $PM_{2.5}$, which made up approximately 18% of the total aerosol (7.3 μg m^{-3}, 4.1 μg m^{-3}), were relatively lower than other cities, such as Prague, Europe (2.9 μg m^{-3}, 2.2 μg m^{-3}, 33%) and Kanpur, India (SO_4^{2-}, 19 μg m^{-3}; NO_3^-, 7.3 μg m^{-3}, 26%), implying that secondary aerosols may have a higher contribution in these cities (Yang et al., 2011). The sulfur oxidation rate (SOR) and nitrogen oxidation rate (NOR) were 0.1 and 0.05 respectively, which indicated lower sulfate and nitrate in atmospheric aerosols compared with other regions (Li and Zhang, 2016). Therefore, the lower content of secondary species in Hohhot indicates that the low concentration of secondary aerosols was attributed to local formation, industrial production, and regional transport (Yang et al., 2011).

Table S2 displays the concentrations of gas-phase precursors in Hohhot and other megacities (Beijing, Tianjin, Guangzhou, Chengdu) in China. It is evident that the level of SO_2 in Hohhot was relatively higher than other megacities which may be related to the large-scale plants. Moreover, the concentrations of NO_2 and O_3 were lower than the concentrations in other megacities. The level of SO_2 in Hohhot was higher than other cities while SO_4^{2-} was relatively lower; the ratios of SO_4^{2-} to SO_2 ranged from 0.11–0.26 for the four seasons. According to several research studies, gaseous precursors (emission from sources), aerosol acidity, and meteorological conditions can influence the formation of SIA. In the following section, the sources, gaseous precursors, aerosol acidity, and meteorological condition are analyzed.

3.2. Source impact analysis of SIA by different models

3.2.1. Characteristics of the emission sources in Hohhot

The identification of pollution sources plays a significant role in source impact analysis. It is important to know the detailed characteristics of different emission sources. Considering source characteristics (source profiles) was essential for the performance of the models, and the profiles of different sources were obtained via the resuspension of source samples collected in Hohhot using the resuspension equipment designed by Nankai University. The details of the suspension sampling device can be found in the Supplementary Information. The profiles were composed of the mass fractions of the chemical components of the different sources' individual profiles. The source profiles of Hohhot can be seen in Fig. S6. Crustal dust consisted mostly of Si (18%), Ca (8.3%), Al (4.0%), and Fe (3.7%); the main components of the coal combustion emissions were OC (12%), EC (6.3%), SO_4^{2-} (14%), Si (15%), and Al (13%). In the cement profile, the fraction of element Ca (44%) accounted for the largest proportion, Si (6.3%) ranked second and Al (2.3%) third. The unique characteristic of vehicle exhaust was its relatively high fraction of OC, which made up 52%. In ambient particulate matter sulfates and nitrates were mainly formed by gaseous SO_2 and NO_X through atmospheric chemical reactions (Pandis and Seinfeld, 1989; Xie et al., 2015) and were mainly present as ammonium sulfate and ammonium nitrate. For the profiles of secondary sulfate and nitrate, this study used the chemical composition of ammonium sulfate and ammonium nitrate as virtual profiles of secondary sulfate and nitrate (Marmur et al., 2005). The profile of SOC was exclusively represented by OC (Lee et al., 2007). In this study, using the inventory of emission sources of Hohhot, crustal dust, coal combustion, cement, and vehicle exhaust may be the primary sources. However, the gaseous precursors emitted by primary sources (coal combustion, vehicle exhaust, etc.) cause the formation of secondary sources including secondary sulfate, secondary nitrate, and secondary organic carbon (SOC) through

Table 1
Species of $PM_{2.5}$ as well as meteorological parameters and gases measured in Hohhot, China.

Species	Percentage in $PM_{2.5}$ (%)	Concentration in $PM_{2.5}$ (μg/m^3)	Summer (μg/m^3)	Autumn (μg/m^3)	Winter (μg/m^3)	Spring (μg/m^3)
Na	1.1	0.8	0.39	0.53	0.84	1.06
Mg	1.2	0.8	0.48	0.62	0.85	1.09
Al	4	2.5	1.25	2.03	3.34	3.63
Si	6.1	3.9	2.08	3.54	3.84	5.79
K	1.7	1.1	0.52	0.84	1.42	1.60
Ca	4.9	2.6	1.90	3.28	3.05	3.15
Ti	0.1	0.07	0.12	0.06	0.07	0.08
V	0.02	0.01	0.20	0.01	0.00	0.00
Cr	0.06	0.05	0.15	0.06	0.04	0.02
Mn	0.06	0.07	0.18	0.04	0.04	0.05
Fe	1.5	1.1	0.48	0.80	1.30	1.38
Ni	0.03	0.04	0.14	0.02	0.02	0.01
Cu	0.09	0.08	0.13	0.05	0.08	0.09
Zn	0.18	0.1	0.12	0.07	0.15	0.12
As	0.01	0	0.07	0.00	0.01	0.01
Pb	0.05	0.06	0.16	0.04	0.03	0.03
OC	18	14	5.34	7.58	18.66	16.02
EC	5.7	4	1.90	3.13	5.03	4.42
NH_4^+	5	3.3	1.88	2.79	4.10	3.46
NO_3^-	6.3	4.1	2.21	3.53	5.04	4.62
SO_4^{2-}	11	7.3	4.63	6.18	8.57	7.73
Cl^-	2.3	1.6	0.65	1.00	2.75	1.74
$PM_{2.5}$	/	66	36.45	52.27	80.54	78.42
SO_2 min	/	/	7.32	10.60	23.64	5.50
SO_2 average	/	/	19.62	36.96	83.14	28.27
SO_2 max	/	/	50.1	94.5	196.7	84
NO_2 min	/	/	19	9.7	13.7	7.9
NO_2 average	/	/	37	47.1	46.1	32.4
NO_2 max	/	/	62.2	87.5	86.4	63.9
T min	/	/	14.0	−8.0	−15.0	−10.0
T average	/	/	20.2	8.0	−8.4	8.3
T max	/	/	27.0	19.0	1.0	23.0
RH min	/	/	32.0	26.0	31.0	13.0
RH average	/	/	52.8	49.0	41.8	35.8
RH max	/	/	87.0	95.0	96.0	80.0

T:°C RH:% WS:m/s.

transformation processes and oxidizing reactions. Thus, secondary sources may also be an important contributor to the local atmosphere pollution.

3.2.2. Source analysis by receptor models

The input dataset of CMB included two parts: one related to the characteristics of six sources profiles including coal combustion, cement, crustal dust, vehicle exhaust, secondary sulfate, and secondary nitrate, and the other contained the main component percentages of receptor data and its corresponding standard deviation including carbonaceous species (OC and EC), water soluble inorganic ions (NH_4^+, SO_4^{2-} and NO_3^-), and inorganic elements (Na, K, Mg, Ca, Al, Si, Ti, Zn, V, Mn, Cu, As, Ni, Cd, Cr, Ba, Fe, Cu, Zn, Pb). There were five divisions of receptor data that represented spring, summer, autumn, winter, and the total year. The input dataset of NCPCRCMB and CMB-Iteration were similar to CMB. As for CMB-GC, the input data include concentration of $PM_{2.5}$, components, uncertainty, sources characteristics (coal combustion, cement, crustal dust, vehicle exhaust, secondary sulfate, secondary nitrate, secondary organic carbon and uncertainty), gaseous pollutants ratio of sources, and the model parameters. A 182 × 19 receptor dataset was introduced in the WALSPMF model to identify the source categories and to quantify its contribution.

The WALSPMF model extracted five factors, and the profiles of the factors calculated by the model are shown in Fig. S7. For Factor 1, there was a large fraction of NO_3^- which is generally considered as the profile of secondary nitrate (Shi et al., 2016). Factor 2 was dominated by SO_4^{2-} and was considered to be the source of secondary sulfate (Tan et al., 2016). It is worth noting that the slight OC also existed in the profiles of secondary sulfate and nitrate. Therefore, the contribution of secondary sulfate and nitrate by WALSPMF might be overestimated. Factor 3 reflected high association with OC and Al which might contribute to coal combustion (Watson et al., 2001). In Factor 4, the signal of Si, Ca, Al, and Fe were distinct, with Si exhibiting the highest loading. These species were the source markers of dust source (crustal and cement) (Kim and Hopke, 2004; Shi et al., 2011a, 2011b). Factor 5 possessed high weight values for organic carbon (OC), element carbon (EC) and NO_3^- which can be regarded as tracers for vehicle exhaust (Shi et al., 2011a; Peng et al., 2016).

The seasonal and annual source impact analysis results resolved by CMB are listed in Fig. S8. There were slight differences between the four seasons. The proportion of the crustal dust was higher in the spring while the coal combustion and vehicle exhaust was higher in winter. The secondary sulfate contribution was greatest in summer (14%) while secondary nitrate contributed more in autumn (9%). The cement contribution (12%) was higher in autumn which was almost three times more than in winter. The source contributions calculated by CMB-GC are displayed in Fig. S9. Overall, coal combustion contributed most in winter; the cement contribution was mostly in autumn; the crustal dust was mostly in spring; secondary sulfate and secondary nitrate were higher in summer and autumn respectively; and there were no significant variations during the year for vehicle exhaust. The percentage contributions of source emissions in four seasons by NCPCRCMB are listed in Table S3. Crustal dust contribution in spring and autumn was relatively higher than in summer and winter which may have resulted from the frequent construction activities in autumn and the higher wind speed in spring. The results from the CMB-Iteration (Fig. S10) were compatible with the aforementioned models. The results estimated by WALSPMF are listed in Table S4. Considering that the principle of FA method was distinct from the CMB models, WALSPMF did not separate the cement from crustal dust clearly; thus the largest contributing source resolved by WALSPMF was dust (32%) (crustal dust and cement). The concentration contributions of the

different sources evaluated with WALSPMF during the four seasons are shown in Fig. S11. Coal combustion played a significant role in winter and spring—the fraction exceeded 20%—with less contribution in the summer and autumn. This phenomenon may be related to the increase in heating demands in winter and early spring. The dust contribution with a fraction of 34% was largest in spring which was mainly from the high incidence of wind-blown dust in spring and continual construction activities during autumn.

The annual percentage contributions indicated by CMB, CMB-GC, NCPCRCMB, CMB-Iteration, and WALSPMF are displayed as follows in Fig. 1: coal combustion (20%, 16%, 22%, 20%, 25%), dust (31%, 25%, 30%, 28%, 32%), vehicle exhaust (14%, 11%, 10%, 11%, 10%), secondary sulfate (11%, 11%, 10%, 10%, 18%), and secondary nitrate (8%, 8%, 8%, 8%, 13%). The contribution of crustal dust and cement were included in the dust category. Overall, the results by all models were reasonable. Considering that WALSPMF can provide daily apportioned results, the results by WALSPMF were used to explore the influence of SIA in the analysis that follows.

3.3. The variations of meteorological factors and gas-phase pollutants

Fig. 2 exhibits the seasonal variations of the meteorological parameters including temperature (T), relative humidity (RH), and wind speed (WS). The seasonal temperature displayed a clear trend with the highest temperatures observed in summer (20 °C). The annual RH was 46%, with summer RH (53%) being higher than autumn (49%), winter (42%) and spring (36%) but was much lower than many megacities (60% in Xi'an, 62% in Tianjin). The wind speed had an opposite trend compared to RH, with an annual speed of 2.9 m/s, and in the spring, seasonal wind speeds were higher than the annual average (3.5 m/s) and lower than the average in summer and autumn (2.6 m/s and 2.7 m/s). The lower RH and higher wind speed in spring followed the anabatic contribution trend of crustal dust developed by the models. The seasonal variations of gas-phase pollutants are also displayed in Fig. 2. The level of CO in winter was clearly higher than in other seasons. The levels of SO_2 and NO_2 in summer (20 μg/m^3, 37 μg/m^3) were lower than in other seasons. Compared to SO_2 and NO_2, the concentration of O_3 (127 μg/m^3) was highest in the summer. As reported in a previous study, higher concentrations of O_3 are usually accompanied by lower gas concentrations (SO_2, NO_2) in warmer months (Zhou et al., 2016).

In the winter, the concentration of SO_2 (83 μg/m^3) significantly exceeded the Chinese annual standard (35 μg/m^3), which was most likely due to coal combustion emission sources. The models quantified that there was higher coal combustion contribution in winter. The seasonal feature of CO was synchronous with SO_2, with CO mainly originating from the incomplete combustion of coal during the heating period. In comparison to the variation of SO_2, the variation of NO_2 was more placid which may correlate with the variations in contributions from vehicle emissions.

Back trajectory analyses were conducted using the TrajStat model for the four seasons. In Fig. S12, it can be seen that in summer the trajectories originated from the south of Hohhot (located in the junction between Shaanxi and Shanxi province) and accounted for 38% of all trajectories which was higher than autumn, winter, and spring (27%, 9% and 14%). Considering the RH in the south was higher and the airflow from south may carry more moisture than from the northwest, the contributions of secondary sulfate were higher in summer. This indicates the important role of RH in the formation of secondary sulfate. In other seasons, the back trajectories were mostly from the dry region, the northwest part of Hohhot (Mongolia and Inner Mongolia), which was not favorable for secondary reactions.

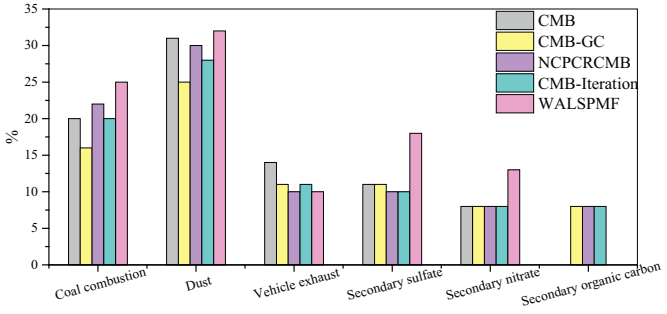

Fig. 1. The annual percentage contributions of multi-models.

3.4. Aerosol pH

Aerosol pH was calculated by ISOPPIRA II (forward mode and "metastable" phase state), and the average level of pH was about 5.6 (with standard deviation 1.7 and range of 1.1 to 8.4). In this study, pH may have been underestimated due to the absence of gas-phase species input (Weber et al., 2016). Compared to the reported fine aerosol pH values in other cities (see Table S5), pH in Hohhot was much higher, which might have been caused by the characteristics of arid regions. Annual crustal dust contributions were about 25% which was much higher than contributions in other cities (such as Beijing and Tianjin (China) and Atlanta and Birmingham (United States)) (Lang et al., 2017; Liu et al., 2017; Verma et al., 2014; Baumann et al., 2008). On the other hand, annual secondary sulfate in Hohhot was only 13%. According to Shi's finding (Shi et al., 2017), dust can increase the particulate pH while secondary sulfate can lower the pH. Therefore, the higher aerosol pH in Hohhot might be reasonable.

The aerosol pH values for all seasons are shown in Table 2. Summer had the highest aerosol acidity (pH is 5.0) followed by autumn (pH is 5.3), winter (pH is 5.7), and spring (pH is 6.1). The pH in summer was lower than in other seasons which were related to the higher contribution of secondary sulfate in summer (17%) than in other seasons (8.7%–15%); therefore, acidic conditions can be attributed to secondary sulfate. The highest pH in spring may be due to the dust periods in spring. The contribution of dust in the spring was 28%, higher than other seasons (range of other seasons 20%–24%). According to other related research (Shi et al., 2017), high levels of some cations (such as Ca^{2+}) from dust can increase the level of aerosol pH.

3.5. Impact of meteorological parameters, gas-phase pollutants, and aerosol pH on SIA

The formation of SIA is significantly influenced by meteorological conditions, precursor emission sources, and the oxidation capacity of the atmosphere (Tan et al., 2016). To investigate the relative influence of meteorological parameters (RH, T) and gas-phase pollutants (SO_2, NO_2, O_3) as well as aerosol pH on secondary aerosol, regression results were analyzed by SPSS. The function among the secondary sulfate concentration and five variables can be described as follows:

$$[SS] = -2.5 + 0.29\,RH + 0.06\,SO_2 + 0.06\,T - 0.12\,pH - 0.03\,O_3 \quad \left(R^2 = 0.25\right) \tag{1}$$

In Eq. (1), [SS] is the concentration (μg/m^3) of the secondary sulfate source estimated by the receptor models. The relationship between secondary sulfate and the five variables is nonlinear so a low R^2 was obtained. The significance level for each variable can be seen in Supplementary Information. Among the five variables, only RH and SO_2 showed the positive relation with sulfate formation. Considering drought conditions in Hohhot, the RH was at a lower level while the SO_2 was at a higher level (in Table S2). Thus, RH may be a key factor for the formation of secondary aerosol. The results agreed with the larger contribution of secondary sulfate in summer since the RH was higher in summer (Table 2). In addition, T may have a positive influence on the formation of secondary sulfate while pH had a negative

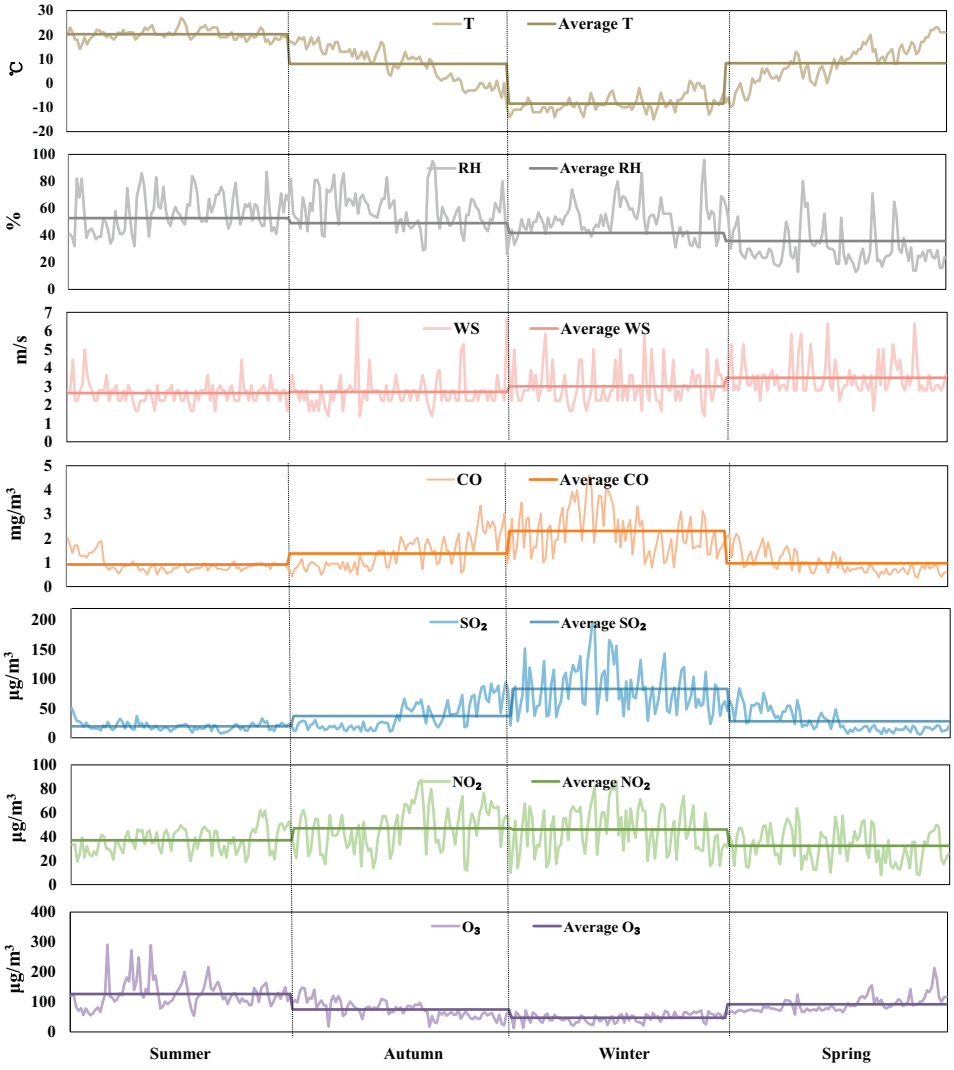

Fig. 2. The seasonal variations of the meteorological parameters and pollutants.

relationship with secondary sulfate. According to Shi's finding (Shi et al., 2017), high secondary sulfate can increase the acidity of the aerosol.

The hydroxyl radical produced by H_2O may be attributed to the oxidation from SO_2 to SO_3 and SO_4^{2-}. In addition, studies have shown that the sensitivity of sulfate to RH may be related to the heterogeneity between clouds and aerosols. Cloud processing is a major source of sulfate at regional and global scales (Luo et al., 2011; Seinfeld and Pandis, 2006). Aerosols can serve as cloud condensation nuclei (CCN) and then can become activated, and soluble gases such as ammonia and sulfur dioxide can dissolve into droplets during the cloud formation. The cloud water can be considered the reacting medium for aqueous-phase reactions, promoting the transformation of dissolved SO_2 to sulfate (Seinfeld and Pandis, 2006). Generally, clouds are classified as precipitating or non-precipitating. Precipitating clouds could be a source or sink of sulfate, and non-precipitating clouds are solely sources of sulfate (Luo et al., 2011). In this study, the high periods of RH may have been caused by the low number of non-precipitating clouds, which lead to the higher sulfate levels.

It is worth noting that some researchers found that NO_2 may contribute to the formation of secondary sulfate (Cheng et al., 2016). However, this phenomenon was rarely observed in this study which may be due to the specific local meteorological conditions in Hohhot. In Fig. 3 (a), higher concentrations of secondary sulfate were closely linked with rising RH as shown in circle 1 (C1). According to related studies, with increasing secondary sulfate, photochemical and liquid phase reactions may occur (Cheng et al., 2016). As shown in circle 2 (C2), the concentrations of secondary sulfate and RH were low while the concentrations of O_3 were in the intermediate level (70–85 μg/m^3),

Table 2
Source contributions of SO_4^{2-}, SO_2, O_3, RH and pH during four seasons.

	Dust* (%)	Secondary sulfate[a] (%)	SO_4^{2-} (μg/m^3)	SO_4^{2-} (%)	SO_2 (μg/m^3)	SO_4^{2-}/SO_2	O_3 (μg/m^3)	RH (%)	pH
Summer	24	17	4.7	13	20	0.24	127	53	5.0
Autumn	24	15	6.4	12	37	0.17	75	49	5.3
Winter	20	12	9.0	10	83	0.11	47	42	5.7
Spring	28	9	7.3	11	28	0.26	92	36	6.1

Dust here means crustal dust.
[a] The average percent contribution of dust and secondary sulfate for each season were estimated by receptor models.

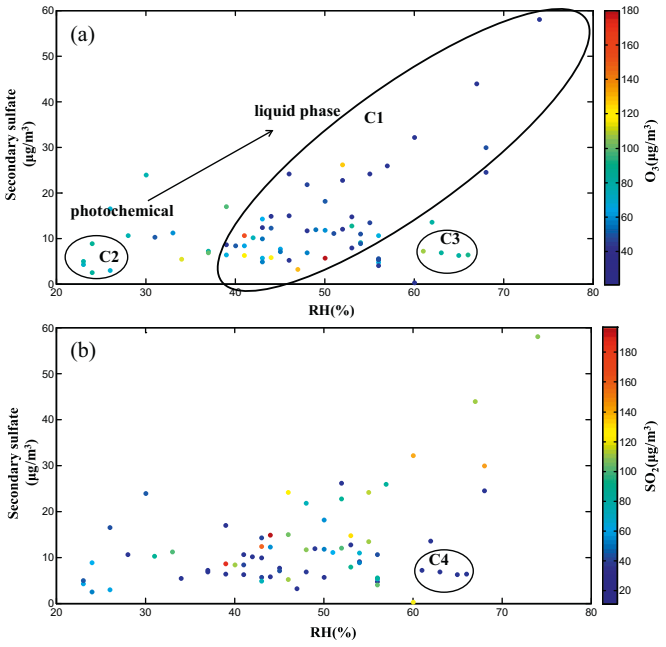

Fig. 3. The relation among secondary sulfate, RH, O_3 and SO_2.

not very high or very low. It is possible that photochemical reactions dominated the samples rather than the liquid phase reaction. When the RH reached a high level, the dominant reaction may have converted to liquid phase reactions. It is worth noting that when the RH reached a high level, the concentration of secondary sulfate was lower, as shown in circle 3 (C3); this may be due to the limited availability of SO_2, as shown in circle 4 (C4) in Fig. 3(b). Additionally, precipitation might be another factor contributing to the low sulfate (points in C3). Overall, RH and SO_2 are found to have the greatest impact on the formation of secondary sulfate, in accordance with our understanding of the chemical pathways that dominate sulfate formation.

Fig. 4 displays the relationship among secondary sulfate, SO_2, and pH. Lower pH is associated with higher secondary sulfate which is consistent with our previous work (Shi et al., 2017). Table 2 shows the comparison among source contributions, SO_4^{2-}, SO_2, O_3, RH, and pH for all seasons. The highest concentration of SO_4^{2-} (9.0 μg/m^3) occurred in winter (compared with other seasons) which may be due to increased emissions from coal combustion (see Figs. S6 & S8). The measured coal combustion profile had a relatively high fraction of SO_4^{2-}, indicating that coal combustion sources also emitted SO_4^{2-}. An interesting finding is that the concentration (μg/m^3) of SO_4^{2-} was lowest in summer (due to the clean conditions in summer), while the percent (%) contribution of secondary sulfate was highest in summer. This may be due to the hydroxyl radical and hydrogen peroxide being higher and other sources

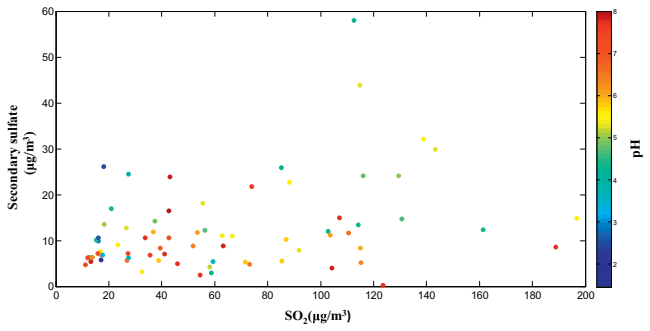

Fig. 4. The relation among secondary sulfate, SO_2 and pH.

are also less intense in summer than other periods, attributing to the formation of secondary sulfate (Seinfeld and Pandis, 2006).

The statistical relationship among secondary nitrate, RH, T and NO_2, pH, and O_3 can be expressed as follows:

$$[SN] = -34 + 0.54\,RH + 0.03\,T + 0.54\,NO_2 + 0.14\,pH - 0.05\,O_3 \quad \left(R^2 = 0.27\right) \tag{2}$$

In Eq. (2), [SN] is the concentration (μg/m^3) of the secondary nitrate source estimated by the receptor models. The significance level for each variable can be seen in Supplementary Information. Similar to Eq. (1), only NO_2 and RH had significant impact on secondary nitrate ($p \leq 0.1$), compared with other variables. RH, NO_2, T, and pH had positive coefficients, suggesting these four items can contribute to secondary nitrate formation. Previous studies showed that high pH may be suitable for the formation of secondary nitrate, and this study was conducted in a nitrate-rich region with high pH (Shi et al., 2017). However, the regression results of secondary nitrate did not fit well due to the high constant term (constant = −34), suggesting that the mechanism of secondary nitrate may be much more complex in comparison to that of secondary sulfate (Seinfeld and Pandis, 2006). For secondary sulfate and nitrate, RH and their gas-phase precursors (SO_2, NO_2) played a vital role in the arid atmosphere.

According to some references (Seinfeld and Pandis, 2006; Cheng et al., 2016), liquid phase reactions are important pathways for the formation of secondary sulfate. These studies focused on aerosol water content. Due to the challenge of measuring water content directly, in this study water content was estimated by ISOPPIRA II (the mode for ISOPPIRA II was same as the mode used for calculating pH). The water content (μg/m^3) was used for regression with secondary sulfate instead of RH and is shown as follows:

$$[SS] = 15 + 0.55\,water + 0.06\,SO_2 + 0.13\,T - 1.5\,pH - 0.03\,O_3 \quad \left(R^2 = 0.33\right) \tag{3}$$

In Eq. (3), water content, SO_2, and pH had a significant impact on secondary sulfate concentrations ([SS]) ($p < 0.05$). The significance level for each variable can be seen in Supplementary Information. Water content and SO_2 had positive coefficients (0.55 and 0.06) while pH had a negative coefficient (−1.5), suggesting that abundant aerosol water content and acidic conditions may be positively associated with secondary sulfate. As discussed above, Hohhot is an arid city with a relatively high aerosol pH (compared to other northern Chinese cities) so it is reasonable that the level of SO_2 in Hohhot was high while SO_4^{2-} was low, as mentioned in Section 3.1. As shown in Table 2, relatively high RH (53%), acidity (pH = 5.0), and higher levels of secondary sulfate (17%) were exhibited in the summer. Low RH (36%) and weaker acidity (pH = 6.1) were exhibited in the spring so the level of secondary sulfate was the lowest in the spring (8.7%).

This paper investigated the relationships (positive or negative) between various factors and secondary inorganic aerosol levels and aerosol acidity. The relationships between secondary sulfate, nitrate, ammonium and other factors are complex. Our analysis relied on linear regression analysis as we tried non-linear regression models, but there was not a substantial improvement, though it is recognized that the chemical mechanisms are non-linear. In the further works, some gases such as NH_3 and HNO_3 should be analyzed, to consider the influence of pH to gas-particle partition.

4. Conclusions

In this study, we selected the arid city Hohhot in China to analyze the influence of meteorological parameters and gas-phase pollutants on SIA formation. The secondary species (SO_4^{2-}, NO_3^-) concentrations in Hohhot were at relatively low levels which may reflect the lower secondary

aerosol concentrations in Hohhot. The pH in Hohhot was about 5.6 which was higher than in other regions reflecting the relatively higher dust contributions in Hohhot. In the summer, pH was lower than in other seasons which were related to the higher contribution of secondary sulfate, whereas higher pH in spring might be connected to the dust periods in the spring. These findings show that relatively higher aerosol pH might exist in an arid atmosphere and influence SIA formation. Further, RH and gas-phase precursors (especially the RH) might be key factors in the formation of SIA. Abundant aerosol water content and acidic conditions were positively associated with the formation of secondary sulfate, while NO_2 and RH had a significant impact on secondary nitrate formation in an arid atmosphere.

Acknowledgements

This study was supported by the National Natural Science Foundation of China (41775149, 1405805), National Key Research and Development Program of China (2016YFC0208500, 2016YFC0208505), Special Scientific Research Funds for Environment Protection Commonweal Section (Nos. 201509020), the Tianjin Research Program of Application Foundation and Advanced Technology (14JCQNJC0810), Tianjin Natural Science Foundation (17JCYBJC23000, 16JCQNJC08700), Fundamental Research Funds for the Central Universities and the Blue Sky Foundation, Fundamental Research Funds for the Central Universities. This publication was developed under Assistance Agreement No. EPA834799 awarded by the U.S. Environmental Protection Agency to Emory University and Georgia Institute of Technology. It has not been formally reviewed by EPA. The views expressed in this document are solely those of the authors and do not necessarily reflect those of the Agency. EPA does not endorse any products or commercial services mentioned in this publication.

Appendix A. Supplementary data

Supplementary data to this article can be found online at https://doi.org/10.1016/j.scitotenv.2018.07.321.

References

Amil, N., Latif, M.T., Khan, F., Mohamad, M., 2016. Seasonal variability of $PM_{2.5}$ composition and sources in the Klang Valley urban-industrial environment. Atmos. Chem. Phys. 16 (8), 5357–5381.

Baumann, K., Jayanty, R.K.M., Flanagan, J.B., 2008. Fine particulate matter source apportionment for the Chemical Speciation Trends Network site at Birmingham, Alabama, using Positive Matrix Factorization. J. Air Waste Manage. Assoc. 58 (1), 27–44.

Cheng, Y., Zheng, G., Wei, C., Mu, Q., Zheng, B., Wang, Z., Gao, M., Zhang, Q., He, K., Carmichael, G., Pöschl, U., Su, H., 2016. Reactive nitrogen chemistry in aerosol water as a source of sulfate during haze events in China. Sci. Adv. 2 (12), e1601530.

Chowdhury, Z., Zheng, M., Schauer, J.J., Sheesley, R.J., Salmon, L.G., Cass, G.R., Russell, A.G., 2007. Speciation of ambient fine organic carbon particles and source apportionment of $PM_{2.5}$ in Indian cities. J. Geophys. Res. 112, D15303.

Fang, T., Guo, H., Zeng, L., Verma, V., Nenes, A., Weber, R.J., 2017. Highly acidic ambient particles, soluble metals, and oxidative potential: a link between sulfate and aerosol toxicity. Environ. Sci. Technol. 51, 2611–2620.

Guo, H., Xu, L., Bougiatioti, A., Cerully, K.M., Capps, S.L., Hite, J.R., Carlton, A.G., Lee, S.H., Bergin, M.H., Ng, N.L., Nenes, A., Weber, R.J., 2015. Fine-particle water and pH in the southeastern United States. Atmos. Chem. Phys. 15 (A9), 5211–5228.

Guo, H., Sullivan, A.P., Campuzano-Jost, P., Schroder, J.C., Lopez-Hilfiker, F.D., Dibb, J.E., Jimenez, J.L., Thornton, J.A., Brown, S.S., Nenes, A., Weber, R.J., 2016. Fine particle pH and the partitioning of nitric acid during winter in the northeastern United States. J. Geophys. Res. Atmos. 121 (17), 10355–10376.

Han, B., Zhang, R., Yang, W., Bai, Z.P., Ma, Z.Q., Zhang, W., 2016. Heavy haze episodes in Beijing during January 2013: inorganic ion chemistry and source analysis using highly time-resolved measurements from an urban site. Sci. Total Environ. 544, 319–329.

Hopke, P.K., 2003. Recent developments in receptor modeling. J. Chemom. 17 (5), 255–265.

Huang, X., He, L., Hu, M., Canagaratna, M.R., Sun, Y., Zhang, Q., Zhu, T., Xue, L., Zeng, L., Liu, X.G., Zhang, Y., Jayne, J.T., Ng, N.L., Worsnop, D.R., 2010. Highly time-resolved chemical characterization of atmospheric submicron particles during 2008 Beijing Olympic Games using an Aerodyne High-Resolution Aerosol Mass Spectrometer. Atmos. Chem. Phys. 10, 8933–8945.

Jaiprakash, Singhai, A., Habib, G., Raman, R.S., Gupta, T., 2017. Chemical characterization of $PM_{1.0}$ aerosol in Delhi and source apportionment using positive matrix factorization. J. Geophys. Res. 24 (1), 445–462.

Kim, E., Hopke, P.K., 2004. Source apportionment of fine particles in Washington, DC, utilizing temperature-resolved carbon fractions. J. Air Waste Manage. Assoc. 54, 773e785.

Lang, J., Cheng, S., Wen, W., Liu, C., Wang, G., 2017. Development and application of a new $PM_{2.5}$ source apportionment approach. Aerosol Air Qual. Res. 17 (1), 340–350.

Lee, S., Russell, A.G., Baumann, K., 2007. Source apportionment of fine particulate matter in the southeastern United States. J. Air Waste Manage. Assoc. 57, 1123–1135.

Li, Y., Zhang, G., 2016. Continuous online observation analysis of water-soluble ions in $PM_{2.5}$ from the atmosphere in spring in Taiyuan. Huanjing Huaxue Environ. Chem. 36, 1777–1784.

Liu, B., Yang, J., Yuan, J., Wang, J., Dai, Q., Li, T., Bi, X., Feng, Y., Xiao, Z., Zhang, Y., Xu, H., 2017. Source apportionment of atmospheric pollutants based on the online data by using PMF and ME2 models at a megacity. China Atmos. Res. 185, 22–31.

Luo, C., Wang, Y.H., Mueller, S., Knipping, E., 2011. Diagnosis of an underestimation of summertime sulfate using the Community Multiscale Air Quality model. Atmos. Environ. 45, 5119–5130.

Marmur, A., Unal, A., And, J.A.M., Russell, A.G., 2005. Optimization-based source apportionment of $PM_{2.5}$ incorporating gas-to-particle ratios. Environ. Sci. Technol. 39 (9), 3245–3255.

Morino, Y., Ohara, T., Yokouchi, Y., Ooki, A., 2011. Comprehensive source apportionment of volatile organic compounds using observational data, two receptor models, and an emission inventory in Tokyo metropolitan area. J. Geophys. Res. 116, 3–25.

Mysliwiec, M.J., Kleeman, M.J., 2002. Source apportionment of secondary airborne particulate matter in a polluted atmosphere. Environ. Sci. Technol. 36 (24), 5376–5384.

Pandis, S.N., Seinfeld, J.H., 1989. Mathematical modeling of acid deposition due to radiation fog. J. Geophys. Res. 94, 12911–12923.

Peng, X., Shi, G., Gao, J., Liu, J., H, Y., Ma, T., Wang, H., Zhang, Y., Wang, H., Li, H., Ivey, C., Feng, Y., 2016. Characteristics and sensitivity analysis of multiple-time-resolved source patterns of $PM_{2.5}$ with real time data using Multilinear Engine 2. Atmos. Environ. 139, 113–121.

Pun, B.K., Seigneur, C., 2001. Sensitivity of particulate matter nitrate formation to precursor emissions in the California San Joaquin Valley. Environ. Sci. Technol. 35 (14), 2979–2987.

Ronneau, C., 1987. Atmospheric chemistry. Fundamentals and experimental techniques. EOS Trans. AGU. 68 (49), 1643.

Sasaki, K., Sakamoto, K., 2005. Vertical differences in the composition of PM_{10} and $PM_{2.5}$ in the urban atmosphere of Osaka, Japan. Atmos. Environ. 39, 7240–7250.

Seinfeld, J.H., Pandis, S.N., 2006. Atmospheric chemistry and physics: from air pollution to climate change. Phys. Today 51 (10), 88–90.

Shi, G.L., Tian, Y.Z., Zhang, Y.F., Ye, W.Y., Li, X., Tie, X.X., Feng, Y.C., Zhu, T., 2011a. Estimation of the concentrations of primary and secondary organic carbon in ambient particulate matter: application of the CMB-iteration method. Atmos. Environ. 45 (32), 5692–5698.

Shi, G.L., Zeng, F., Li, X., Feng, Y., Wang, Y., Liu, G., Zhu, T., 2011b. Estimated contributions and uncertainties of PCA/MLR–CMB results: source apportionment for synthetic and ambient datasets. Atmos. Environ. 45, 2811–2819.

Shi, G.L., Xu, J., Peng, X., Tian, Y.Z., Wang, W., Han, B., Zhang, Y.F., Feng, Y.C., Russell, A.G., 2016. Using a new WALSPMF model to quantify the source contributions to $PM_{2.5}$ at a harbour site in China. Atmos. Environ. 126, 66–75.

Shi, G.L., Xu, J., Peng, X., Xiao, Z., Chen, K., Tian, Y.Z., Guan, X., Feng, Y.C., Yu, H., Nenes, A., Russell, A.G., 2017. pH of aerosols in a polluted atmosphere: source contributions to highly acidic aerosol. Environ. Sci. Technol. 51 (8), 4289–4296.

Shon, Z., Kim, K., Song, S., Jung, K., Kim, N., Lee, J., 2012. Relationship between water-soluble ions in $PM_{2.5}$ and their precursor gases in Seoul megacity. Atmos. Environ. 59, 540–550.

Song, S., Gao, M., Xu, W., Shao, J., Shi, G., Wang, S., Wang, Y., Sun, Y., McElroy, M.B., 2018. Fine particle pH for Beijing winter haze as inferred from different thermodynamic equilibrium models. Atmos. Chem. Phys. 18, 7423–7438.

Squizzato, S., Masiol, M., Innocente, E., 2012. A procedure to assess local and longrange transport contributions to $PM_{2.5}$ and secondary inorganic aerosol. J. Aerosol Sci. 46, 64–76.

Tan, J., Duan, J., Ma, Y., He, K., Cheng, Y., Deng, S.X., Huang, Y.L., Si-Tu, S.P., 2016. Long-term trends of chemical characteristics and sources of fine particle in Foshan City, Pearl River Delta: 2008–2014. Sci. Total Environ. 565, 519–528.

Tian, Y.Z., Liu, G., Zhang, C., Wu, J., Zeng, F., Shi, G., Feng, Y., 2013a. Effects of collinearity, unknown source and removed factors on the NCPCRCMB receptor model solution. Atmos. Environ. 81, 76–83.

Tian, Y.Z., Wu, J.H., Shi, G.L., Wu, J.Y., Zhang, Y.F., Zhou, L.D., Zhang, P., Feng, Y.C., 2013b. Long-term variation of the levels, compositions and sources of size-resolved particulate matter in a megacity in China. Sci. Total Environ. s463–464 (5), 462–468.

Tie, X.X., Huang, R.J., Cao, J.J., Zhang, Q., Cheng, Y.F., Su, Hang, Di, C., Pöschl, U., Hoffmann, T., Dusek, U., Li, G., Worsnop, D.R., O'Dowd, C.F., 2017. Severe pollution in China amplified by atmospheric moisture. Sci. Res. 7, 15760–15767.

Trebs, I., Meixner, F.X., Slanina, J., Otjes, R.P., Jongejan, P., Andreae, M.O., 2004. Real-time measurements of ammonia, acidic trace gases and water-soluble inorganic aerosol species at a rural site in the Amazon Basin. Atmos. Chem. Phys. 4 (4), 967–987.

Trebs, I., Metzger, S., Meixner, F.X., Helas, G., Hoffer, A., Rudich, Y., Falkovich, A.H., Moura, M.A.L., Silva, R.S.D., Artaxo, P., Slanina, J., Andreae, M.O., 2005. The NH_4^+–NO_3^-–Cl–SO_4^{2-}–H_2O aerosol system and its gas phase precursors at a pasture site in the Amazon Basin: how relevant are mineral cations and soluble organic acids? J. Geophys. Res. 110, 1275–1287.

Verma, V., Fang, T., Guo, H., King, L., Bates, J.T., Peltier, R.E., Edgerton, E., Russell, A.G., Weber, R.J., 2014. Reactive oxygen species associated with water-soluble $PM_{2.5}$ in

the southeastern United States: spatiotemporal trends and source apportionment. Atmos. Chem. Phys. 14 (23), 12915–12930.
Wakamatsu, S., Utsunomiya, A., Han, J.S., Mori, A., Uno, I., Uehara, K., 1996. Seasonal variation in atmospheric aerosols concentration covering northern Kyushu, Japan and Seoul, Korea. Atmos. Environ. 30 (13), 2343–2354.
Wang, Y., Zhang, Q., Jiang, J., Zhou, W., Wang, B., He, K., Duan, F., Zhang, Q., Philip, S., Xie, Y., 2014a. Enhanced sulfate formation during China's severe winter haze episode in January 2013 missing from current models. J. Geophys. Res.-Atmos. 119 (17), 10425–10440.
Wang, Y., Yao, Li, Wang, L., Liu, Z., Ji, D., Tang, G., Zhang, J., Sun, Yang, Hu, Bo, Xin, J., 2014b. Mechanism for the formation of the January 2013 heavy haze pollution episode over central and eastern. Sci. China Earth Sci. 57 (1), 14–25.
Wang, Q., Zhuang, G., Huang, K., Liu, T., Lin, Y., Deng, C., Fu, Q., Fu, J.S., Chen, J., Zhang, W., Yiming, M., 2015. Evolution of particulate sulfate and nitrate along the Asian dust pathway: secondary transformation and primary pollutants via long-range transport. Atmos. Res. 169, 86–95.
Watson, J.G., Chow, J.C., Houck, J.E., 2001. $PM_{2.5}$ chemical source profiles for vehicle exhaust, vegetative burning, geological material, and coal burning in Northwestern Colorado during 1995. Chemosphere 43 (8), 1141–1151.
Weber, R.J., Guo, H., Russell, A.G., Nenes, A., 2016. High aerosol acidity despite declining atmospheric sulfate concentrations over the past 15 years. Nat. Geosci. 9 (4), 282–285.
Xie, Y., Ding, A., Nie, W., Mao, H., Qi, X., Huang, X., Xu, Z., Kerminen, V.M., Petäjä, T., Chi, X., Virkula, A., Boy, M., Xue, L., Guo, J., Sun, J., Yang, X., Kulmala, M., Fu, C., 2015. Enhanced sulfate formation by nitrogen dioxide: implications from in-situ observations at the SORPES Station. J. Geophys. Res. 120, 12679–12694.
Xue, J., Lau, A.K.H., Yu, J.Z., 2011. A study of acidity on $PM_{2.5}$ in Hong Kong using online ionic chemical composition measurements. Atmos. Environ. 45 (39), 7081–7088.
Xue, J., Yuan, Z.B., Griffith, S.M., Yu, X., Lau, A.K.H., Yu, J.Z., 2016. Sulfate formation enhanced by a cocktail of high NOx, SO_2, particulate matter, and droplet pH during haze-fog events in megacities in China: an observation-based modeling investigation. Environ. Sci. Technol. 50 (14), 7325–7334.
Yang, F., Tan, J., Zhao, Q., Du, Z., He, K., Ma, Y., Duan, F., Chen, G., Zhao, Q., 2011. Characteristics of $PM_{2.5}$ speciation in representative megacities and across China. Atmos. Chem. Phys. 11 (11), 5207–5219.
Zhai, X., Russell, A.G., Sampath, P., Mulholland, J.A., Kim, B.U., Kim, Y., D'Onofrio, D., 2016. Calibrating R-LINE model results with observational data to develop annual mobile source air pollutant fields at fine spatial resolution: application in Atlanta. Atmos. Environ. 147, 446–457.
Zhang, R., Jing, J., Tao, J., Hsu, S.C., Wang, G., Cao, J.C., Lee, C.S.L., Zhu, L., Chen, Z.M., Zhao, Y., Shen, Z., 2013. Chemical characterization and source apportionment of $PM_{2.5}$ in Beijing: seasonal perspective. Atmos. Chem. Phys. 13 (14), 7053–7074.
Zhou, H.J., He, J., Zhao, B., Zhang, L., Fan, Q., Lü, C., Dudagula, Liu, T., Yuan, Y., 2016. The distribution of PM_{10} and $PM_{2.5}$ carbonaceous aerosol in Baotou, China. Atmos. Res. 178, 102–113.